Journal of Petroleum Science and Engineering 196 (2021) 107786

Contents lists available at ScienceDirect

Journal of Petroleum Science and Engineering

journal homepage: http://www.elsevier.com/locate/petrol

Influence of low-frequency oscillatory motion on particle settling in Newtonian and shear-thinning non-Newtonian fluids

Maduranga Amaratunga *, Herimonja A. Rabenjafimanantsoa, Rune W. Time

Department of Energy and Petroleum Engineering, University of Stavanger, Norway

ARTICLE INFO

Keywords:
Oscillatory motion
Particle settling
Velocity reduction
Non-Newtonian fluids
Shear rate
Drag force

ABSTRACT

An experimental study is performed to observe the effect of vertical fluid oscillations on the mean settling velocity of single spherical glass particles released into mixtures of water and polymeric fluids which exhibit shear-thinning behavior for "non-zero" shear rates. The influence of the shear region in shear-thinning non-Newtonian fluids on the settling rate of spherical particles at different oscillatory conditions is also discussed.

A transparent, U-shaped pipe with a circular cross-section of 50 mm inner diameter is used. Visualizations are captured along one of the two vertical branches of the pipe while a piston generates pressure gradient oscillations in the other branch at three different low frequencies (0.25, 0.5, and 0.75 Hz). Tests at still fluid are also carried out for comparison. Four fluids are considered: water and three mixtures of water-based polymeric solutions which provide the mixture with viscoelastic properties and shear-thinning behavior. Spherical particles of diameter $d = 1$ mm, 2 mm, and 3 mm are released at three different distances from the center of the cross-section: 0, 0.5 R, and 0.8 R, where R is the pipe radius. Particles are released one-by-one and their trajectory is captured from the high-speed camera.

The settling velocity was found smaller if particles were released close to the pipe wall, independently on the rheology of the fluid. A significant reduction of the settling velocity was observed in the presence of an oscillatory flow when a fluid characterized by shear-thinning viscosity is used. According to the results, it was found that the liquid oscillations brought a decrement of up to 7% in the average settling velocity in Newtonian fluid and a 23% decrement of that in non-Newtonian fluids. Moreover, when the fluid oscillates, the shear-layer associated with the particle wake and the pipe wall does not result in any reduction of the settling velocity. In other words, the effect of the near-wall shear layer, which reduces the viscosity of shear-thinning fluids, dominates over the other effects that would not keep the particle longer in suspension.

1. Introduction

After the first introduction of Stokes law for the creeping flow regime by George Stokes in 1851, many researchers have worked a lot on settling of particles in Newtonian fluids even in higher Reynolds numbers (Clift et al., 1978; Khan and Richardson, 1987; Haider and Levenspiel, 1989; Chhabra et al., 1999; Kehlenbeck and Felice, 1999; Brown and Lawler, 2003; Zhiyao et al., 2008; Cheng, 2009). Even the works related to the settling of particles in shear-thinning non-Newtonian fluids are also omnipresent in the literature (Sharma, 1979; Shah, 1982, 1986; Acharya, 1986; Jin and Penny, 1995; Kelessidis, 2004; Malhotra and Sharma, 2012; Arnipally and Kuru, 2018). However, all the above-mentioned studies are related to the settling of particles in stationary fluids while dynamic settling (Harrington et al., 1979; Van Den Brule and Gheissary, 1993; Becker et al., 1994; Childs et al., 2016) has become an interesting topic concerning its practicality and the importance in industrial applications.

Particle settling in oscillatory systems is a practically important example under dynamic settling. Sinusoidal oscillatory fluid motion exhibits a condition of continuously changing acceleration and thus the flow patterns and drag phenomena could be significantly different from those at steady state. Theory and experiments have shown that oscillating or continuously accelerating such systems could exhibit a variety of complicated flow phenomena (Amaratunga et al., 2019b) including periodic vortex shedding (Schöneborn, 1975; Herringe, 1976), boundary layer separation, secondary streaming and wake turbulence (Tunstall and Houghton, 1968), etc.

When talking about the particle settling, it is important to have a fundamental understanding of the comprehensive picture of the forces

* Corresponding author.
E-mail address: amaratunga.maduranga@uis.no (M. Amaratunga).

https://doi.org/10.1016/j.petrol.2020.107786
Received 21 March 2020; Received in revised form 10 August 2020; Accepted 11 August 2020
Available online 16 August 2020

Notations

CMC	Carboxymethyl Cellulose
CFD	Computational Fluid Dynamics
HV	High viscous
LVE	Linear viscoelastic range
MV	Medium viscous
NNF	Non-Newtonian fluid
PAC	Poly-anionic Cellulose
PIV	Particle Image Velocimetry technique
ROI	Region of interest
SAOS	Small amplitude oscillation shear
a	Displacement amplitude of the piston
$a^{'}$	Displacement amplitude of the oscillation (in liquid medium)
A	Amplitude ratio based on the displacement amplitude of the piston
$B(t)$	Basset term
d	Diameter of the spherical particle
C_D	Drag coefficient at oscillatory conditions
C_{D0}	Drag coefficient at stationary conditions
$C_{D0-correlation}$	Drag coefficient of particles at stationary conditions based on the correlation presented in (Morrison, 2013; Morrison, 2016)
D	Diameter of the pipe
f	Frequency of oscillation, Hz; $\omega/2\pi$
g	Gravitational acceleration
Ga	Galileo number
G'	Elastic (or storage) modulus
G''	Viscous (or loss) modulus
K	Consistency index of the non-Newtonian fluid
n	Behavior index for the non-Newtonian fluid
R	Radius of the pipe
t	Time
v_p	Instantaneous velocity of the particle taken as positive downwards
v_{p0}	Terminal settling velocity of the particle at stationary conditions
$\overline{v_{ps}}$	Stationary velocity component within the relative velocity of the particle under oscillatory conditions
v_{pp}	Periodic velocity component within the relative velocity of the particle under oscillatory conditions
v_f	Velocity of the fluid medium taken as positive downwards
R^2	R-squared value of the linear curve fitting
Re_p	Particle Reynolds number in oscillatory conditions
Re_{p0}	Particle Reynolds number in stationary conditions
Re_δ	Oscillatory Reynolds number of the liquid medium

Greek Letters

β	Velocity ratio; v_p/v_{p0}
γ	Strain
$\dot{\gamma}$	Shear rate
ω	Angular frequency; $2\pi f$
λ	Relaxation time of the (slightly viscoelastic) non-Newtonian fluid
μ_f	Dynamic viscosity of the fluid medium
μ_{PL}	Viscosity predicted by the power-law model
ρ_p	Density of the particle
ρ_f	Density of the oscillating fluid (continuous phase)
χ	Added mass coefficient

which results from the fluid on the particles, namely, lift, drag, and buoyancy (Fischer et al., 2002; Zeng et al., 2009). When a spherical particle is moving steadily in a stagnant fluid medium, the forces exerted on the particle can be predicted from the well-known drag coefficient-Reynolds number relationship since the terminal settling velocity occurs when the net gravitational force (gravity minus buoyancy) equals the drag force. However, if the same particle is allowed to settle through an unsteady fluid medium, the contribution of the lift and drag forces to the dynamics of the particles becomes much more significant (Fischer et al., 2002; Cherukat and Mclaughlin, 1994; Lee and Balachandar, 2010) as a result of the changes in the flow patterns around the particle. Those will eventually have a considerable impact on both the instantaneous relative velocity of the particle to the fluid and also on the mean transport velocity of the particle (Herringe and Flint, 1974).

The settling velocity of particles suspended in vibrating/oscillating liquids is of great importance in a wide variety of natural geophysical environments and industrial applications including drilling. According to (Baird et al., 1967), low-frequency oscillations have been used nearly for two centuries in the processing of mineral ores. There are many instances where devices have been used to disperse particles such as bubbles, droplets, and solid particles in liquids by shaking or vibrating the mixtures. The dynamic behavior of such particles in the oscillating continuous phase can impose a significant effect on mass or heat transfer characteristics of the resulting two-phase systems or on mixing and separation in particle-fluid systems (Harbaum and Houghton, 1960; Bailey, 1974; Still, 2012). Ultrasonic fields with short wavelengths are used to enhance mixing to increase the interfacial area in pulse liquid-liquid extraction columns. Furthermore (Bailey, 1974), states that periodic flow pulsations could be used to accelerate ore flotation as well as to speed-up the particle deposition in settling tanks if quick settling is preferred (Singh et al., 1991). mention that the settling of spheres suspended in non-Newtonian fluid with yield stress under the influence of vibrations is of great practical importance while transporting liquid food systems such as soups, sauces, and jams.

1.1. Past work related to particle settling in oscillatory flow

Interest in the geophysical as well as in the industrial problems has spawned many theoretical and experimental studies on particle settling in oscillatory Newtonian fluids in the past. Such studies reveal that the drag forces in unsteady systems tend to exceed the average forces that might be expected from the laws of drag under steady conditions (Bailey, 1974). That means, due to the increased drag forces, the settling velocity of particles in oscillatory fluid systems could be reduced (Tunstall and Houghton, 1968; Hwang, 1985; Ikeda and Yamasaka, 1989) and thus the settling velocity under oscillatory conditions is less than the terminal settling velocity under stationary conditions.

In a fascinating series of papers (Houghton, 1963, 1966, 1968), Houghton describes deeply about the velocity profile around a particle in a sinusoidal field and introduces a hydrodynamic model based on the non-linear Langevin equation to predict the directional motion of particles by applying a sinusoidal velocity to the continuous phase in which the particles are suspended. Thereafter, (Herringe and Flint, 1974), have studied the free fall of particles through a vertically oscillated Newtonian fluid both theoretically and experimentally and state that the motion of the particle is most accurately predicted when the 'history' and 'added mass' terms are preceded by empirical coefficients which are functions of the instantaneous acceleration number.

1.1.1. Mechanism of retardation

If we consider a vortex free situation, based on the non-linear Langevin equation presented by (Houghton, 1963), the motion of a

spherical particle settling in a vertically unsteady flow can be written as;

$$(\rho_p + \chi\rho_f)\frac{\pi d^3}{6}\frac{dv_p}{dt} = (\rho_p - \rho_f)g\frac{\pi d^3}{6} - \frac{1}{2}\rho_f C_D\frac{\pi d^2}{4}(v_p - v_f)|v_p - v_f| + \rho_f\left(1+\chi\right)\frac{\pi d^3}{6}\frac{dv_f}{dt} + B\left(t\right) \quad (1)$$

where, ρ_p is the density of the particle, ρ_f is the density of the oscillating fluid (continuous phase), d is the diameter of the spherical particle, v_p is the instantaneous velocity of the particle taken as positive downwards, v_f is the velocity of the fluid taken as positive downwards, g is the gravitational acceleration, C_D is the drag coefficient, t is the time, χ is the added mass coefficient and $B(t)$ is the Basset term. It is assumed that the continuous phase experiences a uniform velocity (v_f), which is sinusoidal with an angular frequency of ω in the direction of particle motion so that,

$$v_f(t) = a^{'}\omega\cos(\omega t), \quad (2)$$

where, $a^{'}$ is the displacement amplitude of the oscillation. The term on the left-hand side of Eq. (1) represents the inertial forces on the particle. The added mass coefficient (χ) is required to account for the virtual mass that is slightly larger than the ordinary mass of the particle by a fraction of χ of the displaced fluid. In this analysis, χ is taken to be 0.5 (Ikeda and Yamasaka, 1989). The first term on the right-hand side of Eq. (1) gives the buoyancy forces on the particle while the second term represents the frictional (drag) forces on the particle. The third term on the right-hand side of Eq. (1) corresponds to the effects of the pressure gradient in the accelerating fluid phase combined with the virtual mass of the fluid displaced by the particle. According to (Houghton, 1963), the simple form of this term arises from the assumption that there are no velocity gradients in the fluid perpendicular to the direction of motion. The Basset term $B(t)$ has been introduced to allow the effects of deviations of the flow pattern around the particle from that at steady state. If the particle diameter is small and the fluid density is small compared with that of the particle, then $B(t)$ becomes insignificant. Even though ρ_f is not that small compared to ρ_p in this analysis and $B(t)$ is neglected.

The terminal settling velocity of a particle (v_{p0}) in a stationary fluid can be easily derived from Eq. (1) as;

$$v_{p0} = \sqrt{\frac{4}{3}\frac{(\rho_p - \rho_f)}{\rho_f C_{D0}}gd}. \quad (3)$$

Hereafter, the subscript '0' denotes the value in the stationary fluid. If we consider a temporal average of Eq. (1) over a period of fluid motion, with the aid of Eq. (3), it yields (Ikeda and Yamasaka, 1989);

$$C_{D0}.v_{p0}^2 = \overline{C_D\,(v_p - v_f)|v_p - v_f|}. \quad (4)$$

The overbar hereafter denoting temporal averaging over a period of fluid oscillation. From Eq. (4), it can be easily derived that the temporally averaged settling velocity of spheres in a sinusoidally oscillating fluid is equal to that in a stationary fluid as long as the fluid drag obeys Stokes' law. The relative velocity ($v_p - v_f$) can be divided into two parts as a stationary velocity component ($\overline{v_{ps}}$) and a periodic velocity component (v_{pp}). Here, v_{pp} is a function of phase ωt and has following characteristics (Ikeda and Yamasaka, 1989): (i) it is a periodic function with a period of $2\pi/\omega$, (ii) the functional dependence on phase ωt is not given in terms of a simple harmonic but is rather skewed in time and (iii) the temporal average over one-period vanishes (since $\overline{v_{ps}}$ takes up the averaged effect). Therefore, ($v_p - v_f$) can then be written as;

$$v_p - v_f = \overline{v_{ps}} + v_{pp}. \quad (5)$$

For derivation, consider another limiting case for which the instantaneous Reynolds number is always sufficiently large (> 1000) to obey Newton's law of resistance. So, it can be written as (Ikeda and Yamasaka, 1989);

$$C_D = C_{D0} \approx 0.4. \quad (6)$$

With the help of Eq. (6), we substitute Eq. (5) into Eq. (4) and yields;

$$C_{D0}.v_{p0}^2 = C_{D0}\left[\overline{v_{ps}}^2 + \overline{v_{pp}^2}\right]. \quad (7)$$

Based on Eq. (7), it can be concluded that $v_{p0} > \overline{v_{ps}}$ and the settling velocity of particles is caused by the nonlinearity of the fluid drag and the particles exhibit a retardation in oscillatory environments.

However (Baird et al., 1967), state that the reduction of the settling velocity at oscillatory conditions is due to the shedding of a large wake during each oscillation. That shedding replaces the relatively small vortices which are periodically shed from spheres moving steadily. Moreover, the resisting force opposing the motion of a sphere could be attributed to the break-off of the eddies alternately on either side of the sphere in a periodic manner that exerts a periodic force on the particle (Uhlmann and Dušek, 2014; Mazzuoli et al., 2014, 2019). According to the study performed by (Hwang, 1985), the three major factors that govern the variation of effective fall velocity of particles in oscillating flows are the terminal velocity Reynolds number (Reynolds number of the settling sphere in still fluid), the velocity amplitudes of the flow and particle oscillations and the phase lag. However (Ikeda and Yamasaka, 1989), replace the phase lag by the dimensionless frequency of the fluid oscillation and state that an increase of any parameter would increase the retardation of the particle settling. The terminal velocity Reynolds number of the particle ($Re_{p0} = \rho_f v_p d/\mu_f$) is not the same as the instantaneous particle Reynolds number (Re_p) in oscillatory conditions which can be explained as (Boyadzhiev, 1973; Schöneborn, 1975);

$$Re_p = \frac{\rho_f(v_p - v_f)d}{\mu_f}, \quad (8)$$

where, μ_f is the dynamic viscosity of the fluid medium. However, based on the simple conceptual basis provided by (Bailey, 1974) for the particle retardation in oscillatory Newtonian fluid flows, he claims that the settling velocity of the particle can be altered either positively or negatively from its value in steady flow by imposing a "well designed" oscillatory motion on it. The oscillatory motion should have its largest velocity in the direction of the preferred particle motion.

1.2. Significance for non-Newtonian fluids

The related literature mentioned above suggests that the liquid oscillation would retard settling, but the problem of a particle that is free to move in an oscillating fluid is more complicated than we expect. More importantly, when the continuous oscillating fluid is non-Newtonian, the oscillatory motion could generate different shear regions within the pipe area that make the scenario more complicated. When a relatively dense particle settles through a sheared flow in a non-Newtonian fluid, the shear rate of the background flow varies and thus the settling velocity of that particle may vary spatially and temporally due to the non-linear rheology of the fluid. Significant measures to be taken into account with this regard such as the distance that those particles can be transported before settling out, the time they take to do so and the geometry of the deposit, etc.

According to the experimental study performed by (Van Den Brule and Gheissary, 1993), the settling velocity of spherical particles at stationary conditions is reduced by the elastic effects of the non-Newtonian fluid medium due to the presence of normal stress differences and high elongational viscosity. However, in the latter part of their study, they mention about a reduction of the average settling velocity in viscoelastic fluids in the presence of an orthogonal shear-flow field. In a later study (Gheissary and Van Den BRULE, 1996), the same authors extend their experiments to claim that an increment in the settling velocity could be observed with the increase of the shear rate of the main flow of non-Newtonian fluids. This is just because of the non-linear rheology of

the fluids and thus the reduced viscosity with increased shear rate. The same conclusion has been confirmed by (Talmon and Huisman, 2005) with their experimental study on particle settling in viscoplastic fluids under shear flow conditions where the settling velocities increase with increasing shear rate.

In the oil industry, most fracturing/drilling fluids exhibit highly shear-thinning, non-Newtonian fluid characteristics. They are used to suspend drilled cuttings where they expose to different oscillatory conditions while they are circulating through the well or during the solids control operations. They possess completely different properties under shear than when it is at rest. Even though most of the particle settling studies are undertaken in stationary fluids, in the actual drilling process the cuttings are settling while the fluid is moving and mostly oscillating within the fracture. For example, in real drilling operations, the local uneven geometries might induce flow instabilities (Time and Rabenjafimanantsoa, 2013) while the effect of eccentricity in annulus systems is significant in the case of non-Newtonian fluid flow since it may lead to a substantial variation in pressure drop. Generally, the properties of the cuttings being settled, rheology, and density of the drilling fluid, the retardation effect of the confining fracture walls determine the settling rate of cuttings (Malhotra and Sharma, 2012). However, this study proves that the settling of cuttings is governed by the properties of oscillatory motion as well and illustrates the relative importance of studying the settling of particles in non-Newtonian fluids under oscillatory conditions since it is not desirable to have deposition of particles in pipes and boreholes.

1.3. Objective

An extensive and coherent body of information is available for the calculation of drag on spheres settling in quiescent Newtonian and shear-thinning non-Newtonian fluids. However, past work on the determination of settling velocity of particles in a dynamic environment is very limited; out of which any work related to oscillatory motion is sparse.

As mentioned in section 1, low-frequency oscillations are used in several industrial applications, and despite of these practical applications, it appears to be relatively few measurements of particle behavior in non-Newtonian liquids oscillating at low frequencies. The fall velocity of the small particles is affected by the oscillation frequency, shear-thinning, and viscoelasticity of the fluid medium. The effective viscosity of the shear-thinning test liquids varies with the different shear rates results from the oscillation.

In previous publications (Amaratunga et al., 2018, 2019a, 2019b, 2020), the authors clarified the rheological approach to quantify the effect of horizontal and vertical vibration on shear-thinning non-Newtonian polymers, which can be used as model drilling fluids. However, based on the present investigation of single-particle behavior in a vertically oscillating Newtonian and non-Newtonian fluid, it is aimed to bring out valuable conclusions concerning the influence of Newtonian and non-Newtonian liquid oscillations upon the average settling velocity of single particles. Furthermore, it is aimed to provide information on engineering significance in the design of engineering applications experiencing vibration/oscillation and also to understand the mechanics of particle suspension and dislodgement in wall-bounded oscillatory flows.

2. Methodology

The experiments were performed in the multiphase flow laboratory at the University of Stavanger (UiS), Norway.

2.1. Experimental setup

The effect of low-frequency oscillatory motion on particle settling in water and shear-thinning non-Newtonian fluids was investigated in a U-shaped experimental set up as shown in Fig. 1. The test section on the left limb of the U-tube has a circular cross-section with an internal diameter of 50 mm and a total length of 1200 mm. The bottom and the right limbs of the U-tube were also circular in cross-section and 30 mm in internal diameter. The whole U-tube including the piston cylinder (with an internal diameter of 50 mm) was made of transparent acrylic for visualization purposes.

The harmonic oscillations were provided by the piston attached to the right limb of the U-tube, which is driven by a motor-gearbox unit. The rotary motion of the gearbox is converted to a reciprocating motion of the piston by mechanically projecting it into the arm of the piston. The revolution speed of the motor (model: 3DF56-2S7032 from ABM Greiffenberger, Germany) and the gearbox from David Brown (Radicon series), UK was controlled by a frequency controller (model: Micromaster 420 from Siemens) in such a way that, the required output frequency was set to the piston. A tachometer (model: AT-6L from Clas Ohlson, Norway) was used to confirm the frequency of the piston. Experiments with three different oscillation frequencies were tested as 0.25, 0.5, and 0.75 Hz while the tests with still fluid were also performed for the comparison. The length of the rotating arm was fixed in such a way that the resulting oscillation amplitude to be 20 mm. Out of that, the oscillation amplitude ratio (A) was determined as $a/D = 0.4$, where a is the displacement amplitude of the piston, and D is the pipe diameter. An acrylic transparent visualization box filled with deionized water, with dimensions of $15 \times 15 \times 100$ cm^3 was used around the test section to minimize the optical refraction through the curved pipe walls.

2.2. Materials and fluids

2.2.1. Test fluids

Deionized water, being one of the test fluids, was used to prepare three polymeric non-Newtonian Fluids (NNF), later referred to as “Fluid 1”, “Fluid 2”, and “Fluid 3”. They are a mixture of three water-based polymers namely Poly-anionic Cellulose (PAC) called PolyPAC-R provided by MI-Swaco, Norway, medium viscous Carboxymethyl Cellulose (MV-CMC) and high viscous Carboxymethyl Cellulose (HV-CMC) provided by Sigma-Aldrich. The polymer mixtures were mixed using an overhead mixer (Model: Silverson L4RT-A) to ensure proper mixing and allowed more than 72 h to get rid of the trapped air bubbles. The fluid system was optically transparent. The specific details of the polymers and the mixture configuration are mentioned in Table 1.

The viscosity of the NNF was measured by Anton Paar MCR 302 rotational rheometer and the rheological properties are described in section 3.1 with Fig. 5. The density values of the fluids measured using Anton Paar DMA-4500 density meter were 997.55, 999.47, 1000.25, and 1001.01 kg/m^3 for water, Fluid 1, Fluid 2, and Fluid 3 respectively. All experiments were carried out and liquid properties were measured at room temperature of 22 ± 0.5 °C and atmospheric pressure.

2.2.2. Particles

Three different sizes of glass beads were employed in the experiment series to study the settling rate under oscillatory conditions. Accurate particle diameters were measured using an Olympus SZX16 stereomicroscope and an average particle diameter was used in the calculations. The weight of the particles was measured using an analytical balance with digital precision scale and the specific details of the particles used are mentioned in Table 2.

However, the particles will be called with their general sizes (as 1 mm, 2 mm, and 3 mm) for clarity. To cancel out possible effects associated with imperfections of the particle surface, different particles of the same size have been used for each test.

2.3. Experimental procedure

The experimental procedure for this study considered capturing the falling (or rising) of a single spherical particle in a vertical circular

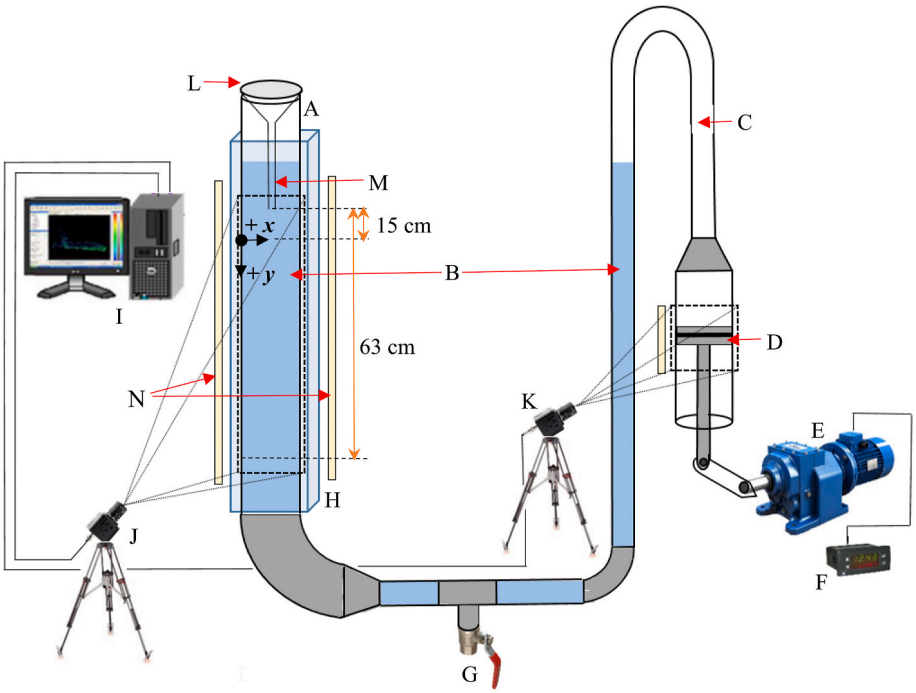

A – Acrylic pipe with ID = 50 mm
B – Test Fluids (Deionized water and non-Newtonian fluids)
C – Air
D – Piston
E – Motor and gearbox
F – Frequency controller
G – Drain valve
H – Transparent box
I – Control PC with frame grabber
J – Camera 1
K – Camera 2
L – Funnel arrangement
M – Dropping tube
N – LED lamps

Fig. 1. Sketch of the experimental setup.

Table 1
Specific details of the polymers and the mixture configuration.

Polymer type	Viscosity at 25 °C	Used weight [g] to dissolve in 5 L of deionized water		
		Fluid 1	Fluid 2	Fluid 3
PolyPAC	800–1200 mPa s (1% H_2O)	0.5	7.5	22.5
MV-CMC	400–1000 mPa s (2% H_2O)	5	5	5
HV-CMC	1500–3000 mPa s (1% H_2O)	4.5	7.5	2.5

Table 2
Specific details of the particles (approx. 50 glass beads).

Particle name	Average diameter [mm]	Average Weight [g]	Density [kg/m^3]
1 mm	1.128 ± 0.003	0.00189 ± 0.0004	2514.9
2 mm	1.986 ± 0.002	0.01111 ± 0.0003	2708.8
3 mm	2.960 ± 0.001	0.03669 ± 0.0002	2701.9

column of fluid that is oscillated in the direction of the particle motion. The primary focus was to study the effects of oscillation frequency on the settling rate without any wall effects. Therefore, the particles were released along the axis of the vertical test section; which was considered as the "Location 1" – (L1). Then, two other locations within the test section which are more closer to the pipe walls were selected (L2 and L3) as illustrated in Fig. 2 to investigate the effect of shear region on particle settling in non-Newtonian fluids. Therefore, L1 ≈ R, L2 ≈ 0.5 R, and L3 ≈ 0.2 R, where R is the pipe radius measured from the pipe wall.

As shown in Fig. 1, a centrally mounted small tube (represented by M in Fig. 1) that was partly immersed in the liquid surface was employed to release the spheres singly into the liquid column. After switching on the driving motor, at least 2 min were left for the oscillatory motion to become harmonic. Then the particles were carefully withdrawn manually into the funnel on top of the dropping tube. The funnel arrangement helped the particle to be directed at the intended dropping location within the test section and the small metal net at the bottom of the dropping tube helped the particle to reduce its initial velocity as low as possible. Therefore, based on the variables, 144 different experimental cases were tested for 4 different frequencies (including still condition), 3 different particle sizes, 4 different fluid types and at 3 different locations within the pipe. All the Newtonian and non-Newtonian fluids were assumed to be incompressible. Each experiment case was repeated three times to achieve a better averaged result and to check the repeatability.

2.3.1. The high-speed imaging system

The motion of the spherical glass beads and their trajectories between two reference points 15 cm and 63 cm below the tip of the dropping tube were captured by a high-speed camera (Camera 1). The y-axis is positive downwards. Some preliminary tests were performed to confirm that all the particle sizes concerned in this experiment achieve their terminal settling velocity at steady conditions before entering this defined boundary. A Basler camera (Model: acA800-510μm USB 3.0 camera with the ON Semiconductor) with a maximum frame rate of 500 fps at a full resolution of 800 × 616 pixel^2 was used for the acquisition of images. Basler lens of model: C125-0818-5 M F1.8 f/8 mm was employed at different frame rates ranging from 25 to 200 fps depending on the speed of the particles in different experimental cases for both

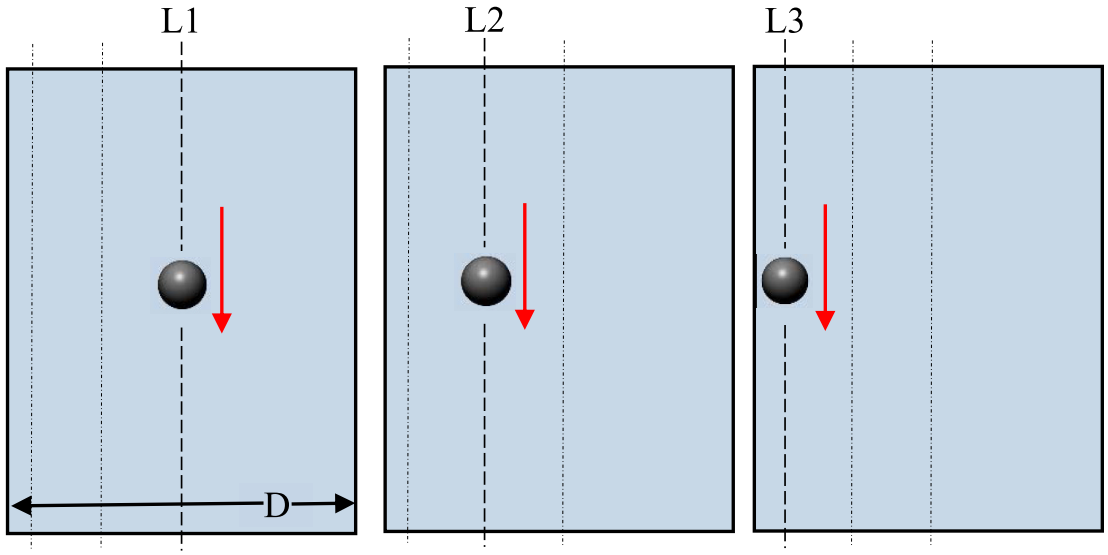

Fig. 2. Particle falling in test fluids at different locations within the test section (the picture is just for the illustration purpose and not in scale).

cameras. The images were cropped to a reduced section of 256 × 616 pixel^2 to fit the view of interest for Camera 1. The two sides of the transparent visualization box were sufficiently illuminated using two LED lamps. Another similar type of a camera (Camera 2) was employed to capture the motion of the piston so that any relation between the particle motion to the piston movement could be interpreted. The view of interest for Camera 2 was 128 × 370 pixel^2. The frame speed of Camera 2 was set identical to Camera 1 and both cameras were synchronized using a LabView program and triggered by a separate control switch. The resulting settling velocities were calculated as described in section 2.3.2. Each experiment case was performed at least three times to ensure consistency and the quality of results. All the experimental cases allocated for a single fluid type were conducted within each day to avoid any inconsistency.

2.3.2. *Data treatment and analysis*

The high-speed image analysis was performed using Tracker – version 4.11.0 (http://physlets.org/tracker/). The whole image was used without specifying any region of interest (ROI) since the full trajectory of the particle is preferred. Specific color adjustments were performed on each image to achieve accurate tracking. Piston movement was also tracked using the same software simultaneously for all the experimental cases incorporating oscillatory conditions.

The characteristic sinusoidal harmonic motion was identified by tracking the displacement of the piston on its vertical plane. Fig. 3 shows a typical sinusoidal movement of the piston together with its phase angle and used as a basis to introduce the notation system adopted by the authors to discuss the results in the latter part of this paper.

The phase position/angle (ωt) was normalized by the angle value ($\pi/4$), and the value for $\omega t/(\pi/4)$ has been utilized in presenting and discussing further results. From the visual observations, great care was taken to release the particle at a moment of the piston movement corresponds to $\omega t/(\pi/4) = 2$ or 10. Once the sinusoidal phase position of the piston is identified and tracked in data analysis, the displacement of the particle is started to track from the moment that corresponds to $\omega t/(\pi/4) = 0$ of the piston movement. Based on the preliminary investigations related to the experiment, the authors verify that both steady and periodic regimes are reached by the particles within the span of the trajectory image frame.

Since the velocity of the particle is fluctuating with the oscillatory motion, it was challenging to determine the velocity of each particle directly. However, the trajectory of any particle is a function of space and its gradient is the instantaneous velocity of it. Therefore, the obtained particle trajectory (vertical component of the displacement) is fitted to a linear curve to achieve its average settling velocity within the test section as depicted in Fig. 4.

According to the specific test conditions depicted in Fig. 4, it can be seen that the trajectories are not 100% straight in the experimental cases

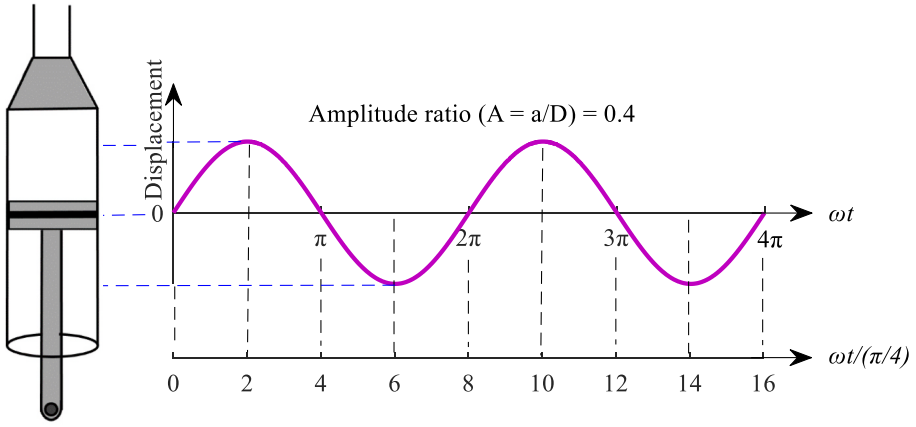

Fig. 3. Introduction of the different phase positions within the oscillation period based on the displacement of the piston.

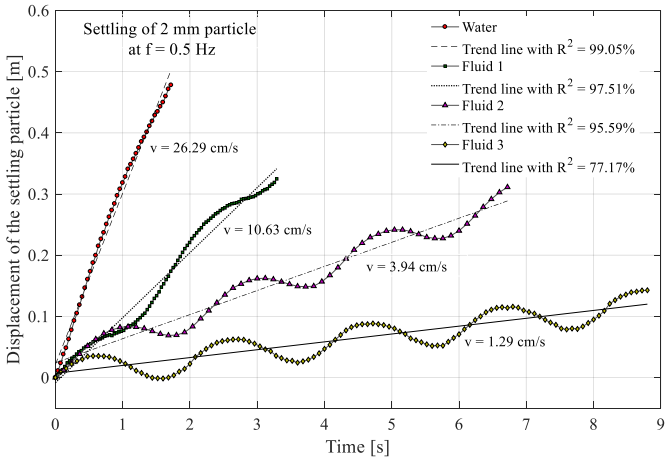

Fig. 4. Illustration of the data treatment and analysis method to achieve the average settling velocity of particles (The trajectories are shown for the whole span of the image frame with time and not based on the phase positions. Number of data points are different due to the different acquisition rates and data filtering in plotting the figure. The y-axis is positive downwards.).

associated with oscillatory motion. Therefore, the error associated with linear curve fitting of the trajectory becomes significant for some experimental cases. This will be discussed separately in section 3.6 under error analysis. The obtained average settling velocities are used to compare the effect of different oscillatory conditions on particle settling rate in Newtonian and non-Newtonian fluids.

It was observed that the particle motion was not oblique for almost 98% of the test cases, but in certain instances, some particles exhibited spiral or rocking motion on traveling down the liquid column. Even though it is interesting in themselves for other studies, such cases were neglected in the data processing. Based on the calculations on the oscillatory Reynolds number (Re_δ) for the same experimental setup and conditions (Amaratunga et al., 2020), it was found that the oscillatory boundary layer close to the pipe wall was laminar in all cases.

3. Results and discussion

The significance of the different test fluids selected for this study in a rheological context and the effect of oscillatory motion on the settling of spherical particles in Newtonian and non-Newtonian fluids are described in the following section.

3.1. Rheology of the fluids

The rheological properties of the non-Newtonian fluids were measured by a modular compact rheometer (Anton Paar – MCR 302), using the concentric cylinder configuration (CC27). Fig. 5 shows the dynamic viscosity (μ) curves for the all the three Non-Newtonian fluids used in the experiment. The power-law rheological model was used to model the viscous and the shear-thinning behavior of the test fluids as shown in Eq. (9);

$$\mu_{PL} = K\dot{\gamma}^{n-1}. \tag{9}$$

Here, μ_{PL} is the viscosity predicted by the power-law model, K is the consistency index, n is the behavioral index and $\dot{\gamma}$ is the shear rate. It is important to mention here, that the power-law model is fitted to the experimental data in the range of shear rates encountered by the particles within all the experimental cases. Also, it does not cover the constant viscosity plateau observed in the low values of shear rate. The shear rate used is the maximum particle shear rate defined as (Shah et al., 2007; Uhlherr et al., 1976);

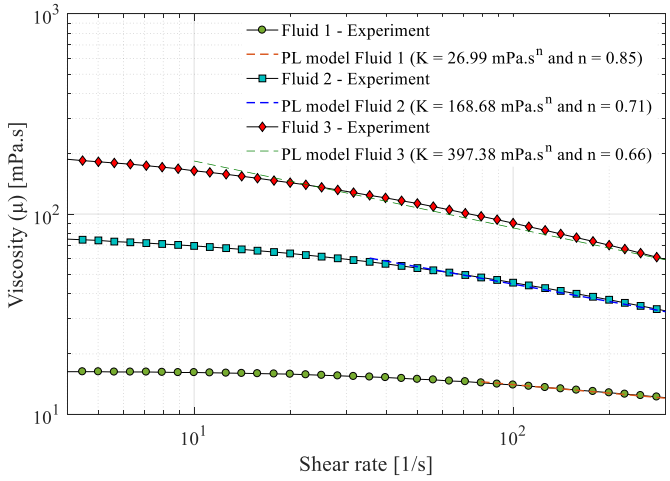

Fig. 5. Viscosity curves for the test fluids at 22 °C.

$$\dot{\gamma} = \frac{3v_p}{d}. \tag{10}$$

The parameters for the model are mentioned in Fig. 5 and also summarized in Table 3. The shear-thinning behavior of the test fluids can be easily distinguished from the viscosity curves where Fluid 3 is the most shear-thinning fluid with the lowest n value. The viscoelastic properties of the test fluids were also measured in small-amplitude oscillation shear (SAOS) tests as part of the rheological investigation. Strain amplitude sweeps (results are not presented in this paper) were conducted to determine the linear viscoelastic (LVE) region of the non-Newtonian test fluids at low strain amplitudes.

The viscoelastic property of the non-Newtonian test fluids in their obtained LVE range was investigated by carrying out frequency sweeps. Fig. 6 shows the results of the frequency sweep test for Fluid 3 over a given angular frequency (ω) range (ramped down logarithmically from 100 to 1 rad/s) at a constant strain 1%.

It can be seen from Fig. 6 that both the storage and the loss moduli increase when the frequency is increased. However, the storage modulus (G') increases faster than the loss modulus (G'') and the elastic behavior of the fluid becomes dominant over its viscous behavior after a certain angular frequency. This particular frequency where $G' = G''$, is termed as the crossover frequency as illustrated in Fig. 6. The inverse of this crossover frequency represents the longest characteristic relaxation time (λ) of the polymer solution (Arnipally and Kuru, 2018) which can be used to quantify the elasticity of the fluid. The corresponding λ values for the three fluids are mentioned in Table 3.

According to the values presented in Table 3, it can be observed that Fluid 1 has the highest relaxation time of the test fluids and therefore has the highest elasticity. Since the λ values after all are very small, it could be concluded that the test fluids are only slightly viscoelastic. All the aforementioned rheological properties were measured just after the corresponding experimental run.

The dynamic viscosity of water was measured to be 0.9544 mPa s at 22 °C.

Table 3
Rheological parameters for the test fluids.

	K [mPa.s^n]	n [-]	λ [s]
Fluid 1	26.99	0.85	0.037
Fluid 2	168.68	0.71	0.019
Fluid 3	397.38	0.66	0.015

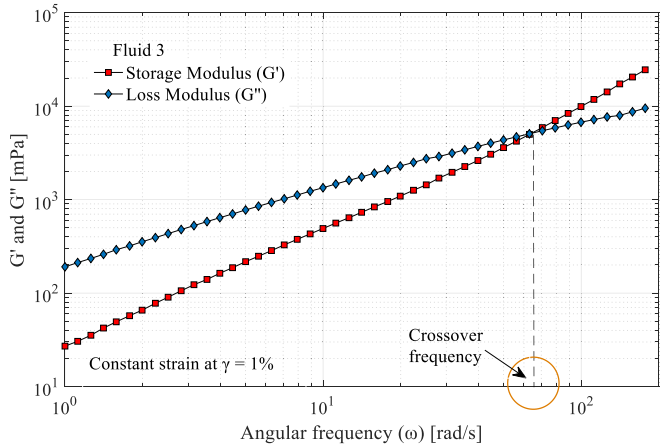

Fig. 6. Frequency sweep test for Fluid 3 at a constant strain at $\gamma = 1\%$.

3.2. Settling velocity at stationary conditions (in quiescent fluid) along pipe axis (location 'L1')

As described in the experimental procedure, the settling of spherical particles was captured by a high-speed camera under stationary conditions before imposing any oscillatory motion. That helped in assessing the experimental data and results of the present analysis in comparison to the well-established knowledge on particle settling in stationary Newtonian and non-Newtonian fluids.

Fig. 7 shows the terminal settling velocities of spherical particles falling in all the test fluids without any oscillatory motion imposed. The particles were carefully released with the help of the dropping tube so that they obtain very little or negligible initial velocity at the beginning. It can be observed in Fig. 7 that the terminal settling velocity of particles within the Newtonian fluid (deionized water) is larger than that within all the other non-Newtonian fluids. This is due to the increased viscosity of non-Newtonian fluids and therefore the increased drag force exerted on the particles. The increased drag effect becomes significant when the non-Newtonian fluids become more viscous and shear-thinning which can be seen from the low terminal settling velocities achieved by the particles settled in Fluid 3 compared with other two NNFs. This reduction of terminal settling velocity could also be attributed to the negative wake that is perceived to happen only in shear-thinning viscoelastic fluids (Maalouf and Sigli, 1984).

Moreover, when the particle diameter is increased the terminal settling velocities show an increasing trend for all the test fluids. However, it can be noticed that the rate of increase in terminal settling velocity (with increasing particle size) is higher for water and low viscous NNFs compared to that with high viscous Fluid 3. This means that larger particles settle down at a slower rate than the smaller particles when the shear-thinning of the NNF is increasing (when n becomes low). From the practical point of view, increasing shear viscosity may be an effective solution to achieve suspensions of large-sized particles.

Many theoretical (Houghton, 1963, 1966, 1968; Herringe and Flint, 1974; Bailey, 1974; Hwang, 1985) and experimental studies (Tunstall and Houghton, 1968; Ikeda and Yamasaka, 1989) have indicated that the proximity to a cylindrical wall can noticeably increase the drag on spheres when the ratio of the particle to the pipe diameter (d/D) exceeds 0.1. However, in the present analysis all the test results taken at Location 'L1' has a value of $d/D < 0.06$. Therefore, it is assumed that the settling velocities obtained at this specific location are free from wall effects. Furthermore (Uhlmann and Dušek, 2014), state that when steady, vertical particle motion is concerned, four basic regimes can be defined based on the Galileo number (Ga) that can be expressed as;

$$Ga = \frac{\sqrt{\left|\frac{\rho_p}{\rho_f} - 1\right| g d^3}}{\nu}. \tag{11}$$

Ga is the ratio of gravity forces to the viscous forces and quantitatively it is less than 300 for all the steady-state test cases except for the settling of 2 mm and 3 mm particles in water. Despite those two outlier cases, all the test runs can be categorized as 'steady vertical' based on the classification provided by (Uhlmann and Dušek, 2014).

3.2.1. Validation of particle tracking method and the experimental results

To validate the experimental measurements captured by the high-speed imaging system, and to prove the accuracy of the particle tracking method, the terminal settling velocities (at quiescent conditions) of the three particles in water at Location 'L1' were used. Based on the terminal settling velocities for those three sizes of glass beads, the drag coefficient was calculated using Eq. (12), which is just a re-arrangement of Eq. (3);

$$C_{D0} = \frac{4}{3} \frac{g d \left(\rho_p - \rho_f\right)}{\rho_f v_{p0}^2}. \tag{12}$$

The terminal velocity Reynolds number of the particle ($Re_{p0} = \rho_f v_p d/\mu_f$) was then calculated as described in section 1.1. The calculated C_{D0} values were plotted upon the drag coefficient ($C_{D0-correlation}$) versus Re_{p0} correlation (Morrison, 2013, 2016) graph as shown in Fig. 8. This correlation is shown in Eq. (13).

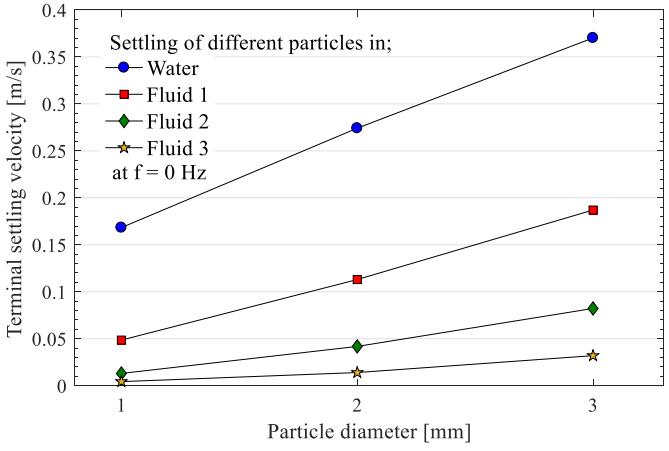

Fig. 7. Terminal settling velocities of spherical particles at stationary conditions.

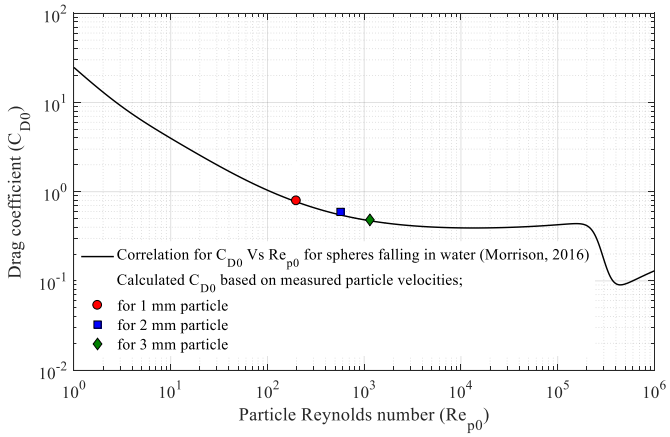

Fig. 8. Drag coefficient versus particle Reynolds number.

$$C_{D0-correlation} = \frac{24}{Re_{p0}} + \frac{2.6\left(\frac{Re_{p0}}{5.0}\right)}{1+\left(\frac{Re_{p0}}{5.0}\right)^{1.52}} + \frac{0.411\left(\frac{Re_{p0}}{263000}\right)^{-7.94}}{1+\left(\frac{Re_{p0}}{263000}\right)^{-8.00}} + \frac{0.25\left(\frac{Re_{p0}}{10^6}\right)}{1+\left(\frac{Re_{p0}}{10^6}\right)}. \quad (13)$$

According to Fig. 8, it can be seen that all the drag coefficient values calculated from experimentally measured terminal settling velocity values (using high-speed imaging technique and the particle tracking method) are within 5% deviation from the data correlation presented by (Morrison, 2013, 2016), which is an acceptable variance.

3.3. Particle displacement in oscillatory conditions along pipe axis (location 'L1')

When a particle is settled in a dynamic environment, it experiences an imbalance in hydrodynamic forces, and it tries to exhibit different falling/rising patterns from that we expect at steady situations. When particles are settled in either stationary or oscillatory conditions, the deviations in their straight vertical path as well as their unsteadiness originate from the characteristics of the fluid motion in the near field around the particle and in its wake (Uhlmann and Dušek, 2014). Tracking the particle displacement is a proven technique to analyze and study the motion particles in unsteady oscillatory conditions while the observation of wake patterns provides more in-depth details regarding the hydrodynamics.

3.3.1. Variation of particle displacement with the frequency of oscillation

The oscillatory motion imposed on the fluid medium was mainly characterized by the driving frequency and the amplitude of the fluid oscillations being fixed. Therefore, it is important to check how the particle moves downwards (or upwards) at different frequencies. Fig. 9 presents the vertical component of the displacement of the spherical particles (1, 2, and 3 mm) in water and Fluid 3 when the fluids are at rest ($f = 0$ Hz) while Fig. 10 presents the same results when the fluids have been oscillated. The three panels of Fig. 10 are drawn based on the notation basis illustrated in Fig. 3, which is basically for a time period of one phase cycle. Diagrams for the displacement evolution for the other two test fluids are not shown for the clarity of the figure. Note again that the y-axis is positive downwards in all Figs. 9–11.

It can be seen that the time development plots of the particle displacement shown in Fig. 9 are pretty straight forward since they were recorded in quiescent conditions. All of them, no matter whether it is Newtonian or non-Newtonian, possess a linear displacement profile along the test section, and determination of their terminal settling velocity is easy. The typical observations for a particle that settles in a quiescent Newtonian (or non-Newtonian) fluid could be seen here. For example, larger particles travel through the image frame faster than the smaller ones indicating they settle faster. The same-sized large particles take a bit extended time to leave the image frame when it is allowed to settle non-Newtonian fluid due to the viscous resistance of the non-Newtonian fluid.

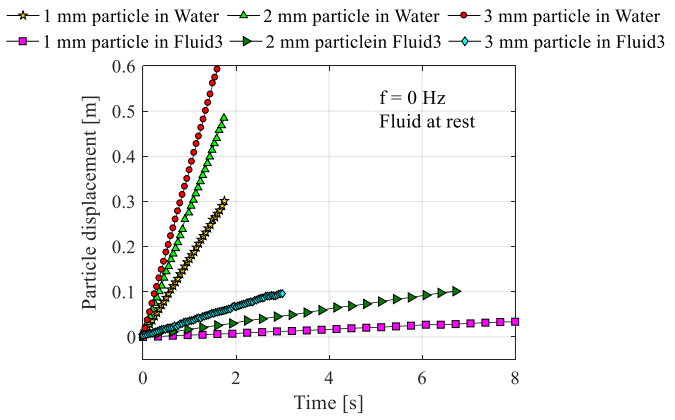

Fig. 9. Vertical component of the particle displacement in water and Fluid 3 when the fluids are at rest (stationary conditions). The y-axis is positive downwards.

However, the displacement profile of the particle when they are allowed to settle in an oscillated fluid medium (see Fig. 10) is different than that at stationary conditions. The vertical displacement of particles in water does not show to be much affected by the oscillation at lower frequencies. When the frequency is increased the displacement curves for water tend to show some response to the oscillatory motion. However, it could be seen that the vertical component of the displacement curves of the particles in non-Newtonian fluids is significantly affected at all frequencies. It seems like particles follow the motion of the continuous non-Newtonian fluid medium than it does in a Newtonian fluid. When the oscillatory motion is present, the frictional force or the drag force together with lift force on the particle act either in the same direction as the buoyancy force or in the opposite direction. The magnitude of each force depends on the viscosity of the fluid medium and the size of the particle.

The slopes of the curves provide the settling velocity of each particle and since in some cases, more than one oscillation period is considered, it could be termed as 'average velocity'. Thus, it could be seen that large-sized particles have achieved higher settling velocities at all the oscillation frequencies and all sized particles tend to settle faster in water than in any non-Newtonian fluid even at oscillatory conditions.

3.3.2. Variation of particle displacement with different fluid types

The displacement profiles shown in Figs. 9 and 10 are only for one period of oscillation. However, it is of interest to know how the particles settle/rise in different test fluids for a bit of longer oscillation time. Therefore, Fig. 11 shows the vertical component of the particle displacement for different fluid types, all the particle sizes, and for the oscillation frequency equal to 0.75 Hz.

According to Fig. 11, it can be seen that the displacement of the particles in water is not affected significantly even at higher frequencies; especially for the large-sized particles. In comparison to that, all particle sizes are greatly affected and influenced by the oscillatory motion in such a way that they alter their displacement direction (vertically as downwards and upwards) from time to time within the oscillation period in the course of settling. Fig. 10 shows that the time development of the vertical displacement is dominated by sub-harmonic oscillations and this could be caused by the phase lag between the particle dynamics and the oscillatory flow due to the particle inertia. According to the plots of displacement evolution of the particles shown in Fig. 11, a condition of partial stability (or stagnation) of the particles could be observed in some instances especially at higher fluid viscosities and also for smaller sized particles. This temporary stability is simply due to the initial relaxation of the particle to align with the action of the combined gravitational force (downwards) and the viscous drag (oscillating). If the liquid was purely oscillating in absence of gravitation the particles would follow nearly the same motion. The only difference would be the particle inertia. If the liquid flowed with constant speed in absence of gravity, the particle would follow more or less completely aligned, except for local liquid perturbations. An alternative but fully equivalent way to depict the motion would be to take the numerical time derivative of the displacement trajectories to give the "falling speed" of the particles. However, we chose to show the displacement as these are the raw data, and the numerical derivative could be too fluctuating. Fig. 4 shows how the trend lines are used to give a steadier estimate.

Moreover, the displacement plots in Fig. 11 reveal that the disturbances to the settling velocity and consequently the possible retardation effect would become significant with increasing viscosity of the test fluids. Indeed, the larger the viscosity, the smaller the Stokes number of settling particles. The relaxation time for particles settling in Fluids 2

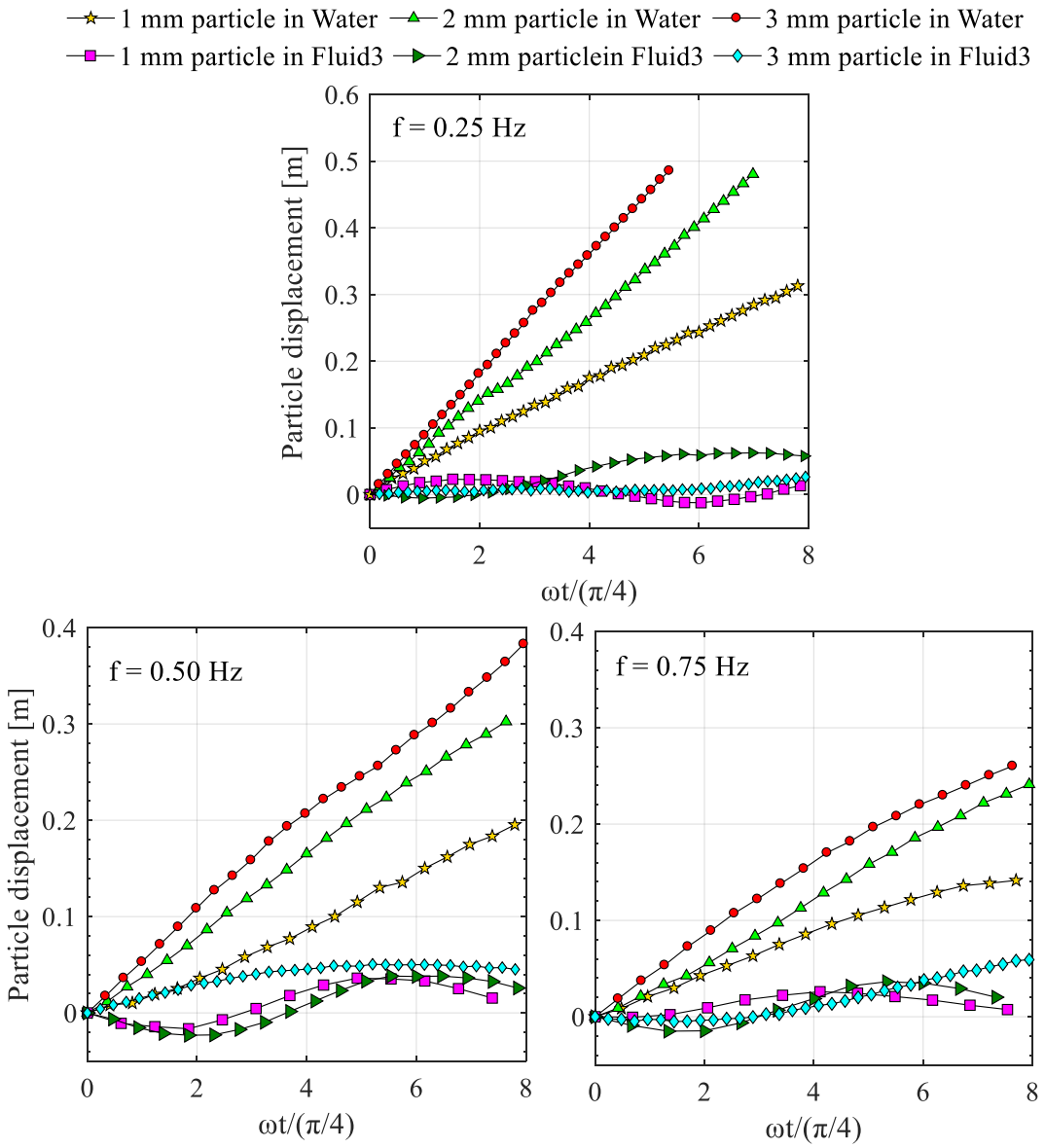

Fig. 10. Vertical component of the particle displacement in water and Fluid 3 at all frequencies. The y-axis is positive downwards.

and 3 is small and particles follow the oscillatory flow. Contextually, the particle Reynolds number is smaller than in the cases with water, and Fluid 1 and correspondingly fluctuations of the fluid velocity around the particle are foreseeably weaker. Therefore, when the particle becomes smaller in size, it possesses a lower amount of buoyancy compared to the drag forces exerted by the continuous liquid medium, and highly viscous fluids would arrest the fall velocities at higher oscillation frequencies.

3.4. Settling velocity of particles in different oscillatory conditions along pipe axis (location 'L1')

As explained in section 2.3.2, the average settling velocity of the particles at different oscillatory conditions was approximated by fitting the vertical component of the displacement profiles of the particles into a linear curve and considering its slope. To provide a clear idea about the changes in settling velocity of particles at each oscillating condition by comparing those with the non-oscillating condition, a velocity ratio (β) is defined as;

$$\beta = \frac{v_p}{v_{p0}}, \tag{14}$$

where, v_p is the average settling velocity of given particle size at a particular oscillation frequency settled along the pipe axis ('L1') in a particular test fluid. Then v_{p0} is selected as the terminal settling velocity (at non-oscillating conditions) of the same sized particle settled along 'L1' within the same test fluid. Fig. 12 shows how β varies with the changing of oscillation frequency for different particle sizes while Fig. 13 shows the same for different fluid types for better understanding.

According to Figs. 12 and 13, it can be observed that the settling velocity of the particles at oscillatory conditions has been reduced from that at stagnant condition except for a couple of outlier values for the combinations of 2 mm particle in Fluid 1 and 1 mm particle in water and Fluid 2. The slight variance in β that can be observed at oscillatory conditions compared to the terminal settling velocities presented in Fig. 7 could be due to the uncertainty effects related to slight variations in particle shape and the exact radial position could perhaps be masked by azimuthal movement. Moreover, it could also be attributed to a condition of adverse pressure-gradient where the wake becomes unstable and fluctuations of the drag force appear even though the flow is laminar for all the test cases based on the oscillatory Reynolds number explained in (Mazzuoli et al., 2014; Amaratunga et al., 2020).

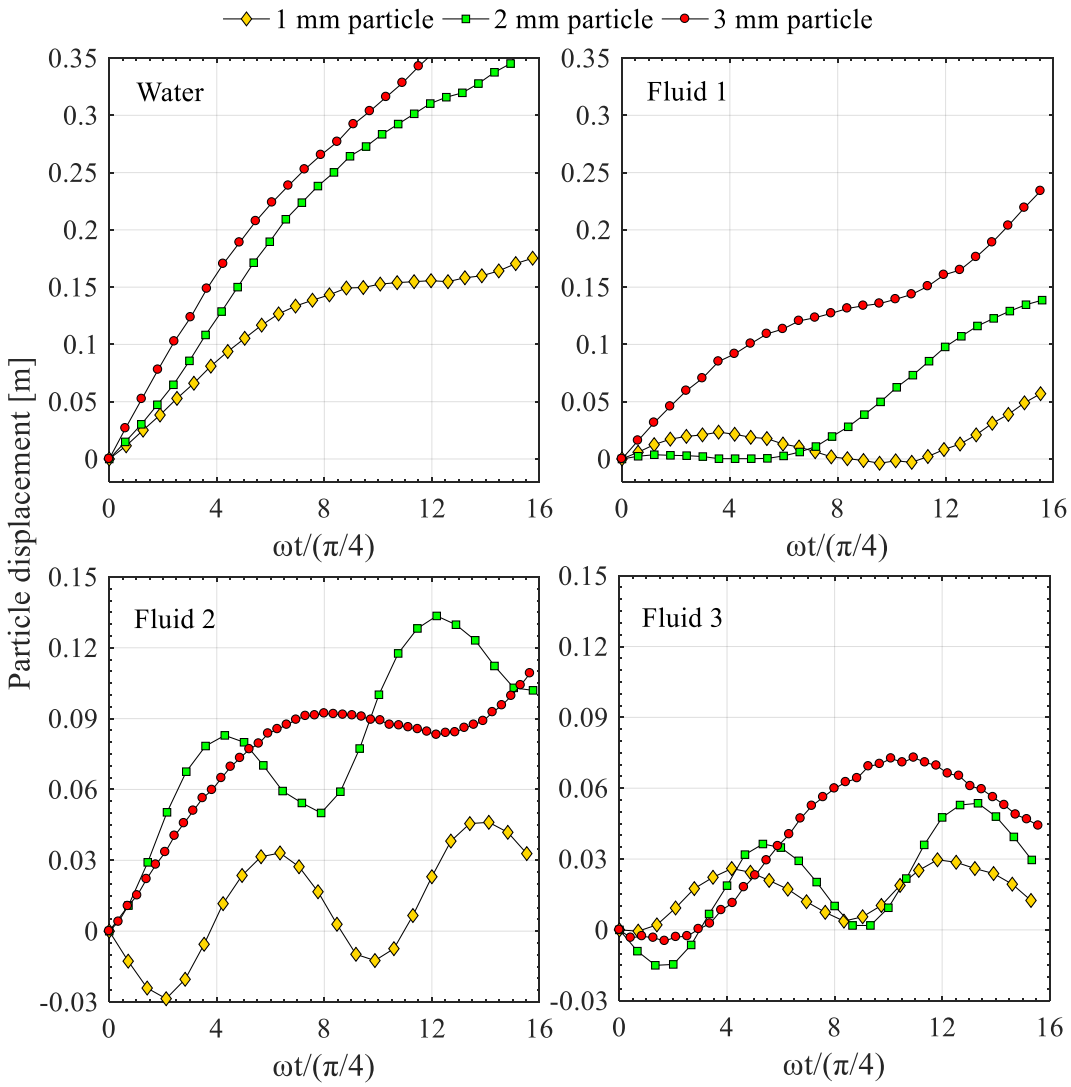

Fig. 11. Vertical component of the particle displacement in all test fluids at f = 0.75 Hz. The y-axis is positive downwards.

However, Figs. 12 and 13 again prove the fact that water being the Newtonian fluid shows the least affected by the oscillations in terms of the velocity reduction while the significance of retardation becomes increased when the non-Newtonian fluids become more viscous with increased shear-thinning effects.

The variation of β within water always lies close to unity, which ranges from 1.05 to 0.92 for all the particle sizes. That indicates that there has been only a slight drag enhancement on the particles due to the oscillations when they are settled in the water. However, a reduction of β in the range from 4 to 23% could be observed in non-Newtonian fluids where the maximum reduction is achieved when the particles are settled in Fluid 3. This reduction of velocity could be attributed to the oscillation-induced increases in the drag coefficient on the particles at unbounded shear conditions and to the unstable wake due to the continuous changing of the oscillatory flow (Zeng et al., 2009). The drag force on the particles in oscillatory conditions is significantly modified by the instantaneous relative velocity between the particles and fluids (Hwang, 1985) because of the continuous flow changes within the flow.

Furthermore (Tunstall and Houghton, 1968), state that the occurrence of any secondary effects such as phase lag, virtual mass, etc. Can also not be negligible with this regard. The existence of fluid inertia and viscosity could lead to a phase lag between the fluid and the particles. The compressibility of the air pocket in between the piston and fluid system has a greater responsibility for this (Houghton, 1966). states that, any technique that can increase the phase lag between particle motion and the motion of displaced fluid would reduce the settling velocity that will eventually increase the hold-up time in two-phase particulate systems. Furthermore, particle inertia is not negligible to that of the fluid in this scenario and the drag coefficient is most likely be affected by the unsteadiness of the wake.

3.5. *Effect of the shear region on settling velocity (settling at 'L2' and 'L3')*

As explained in the introduction, since the unsteady oscillatory pipe flow undergoes flow reversals continuously and thus the axial velocity is varying both in magnitude and direction, the shear rate is time-varying and effects from that become more pronounced for non-Newtonian fluids.

The same approach has been taken as described in Eq. (13) to quantify the effect of walls at stationary conditions and the effect of the shear region at oscillatory conditions. Here the instantaneous settling velocity of the particle (v_p) refers to the value either along 'L2' or 'L3'. v_{p0} is the same as that measured along 'L1' for resting fluid.

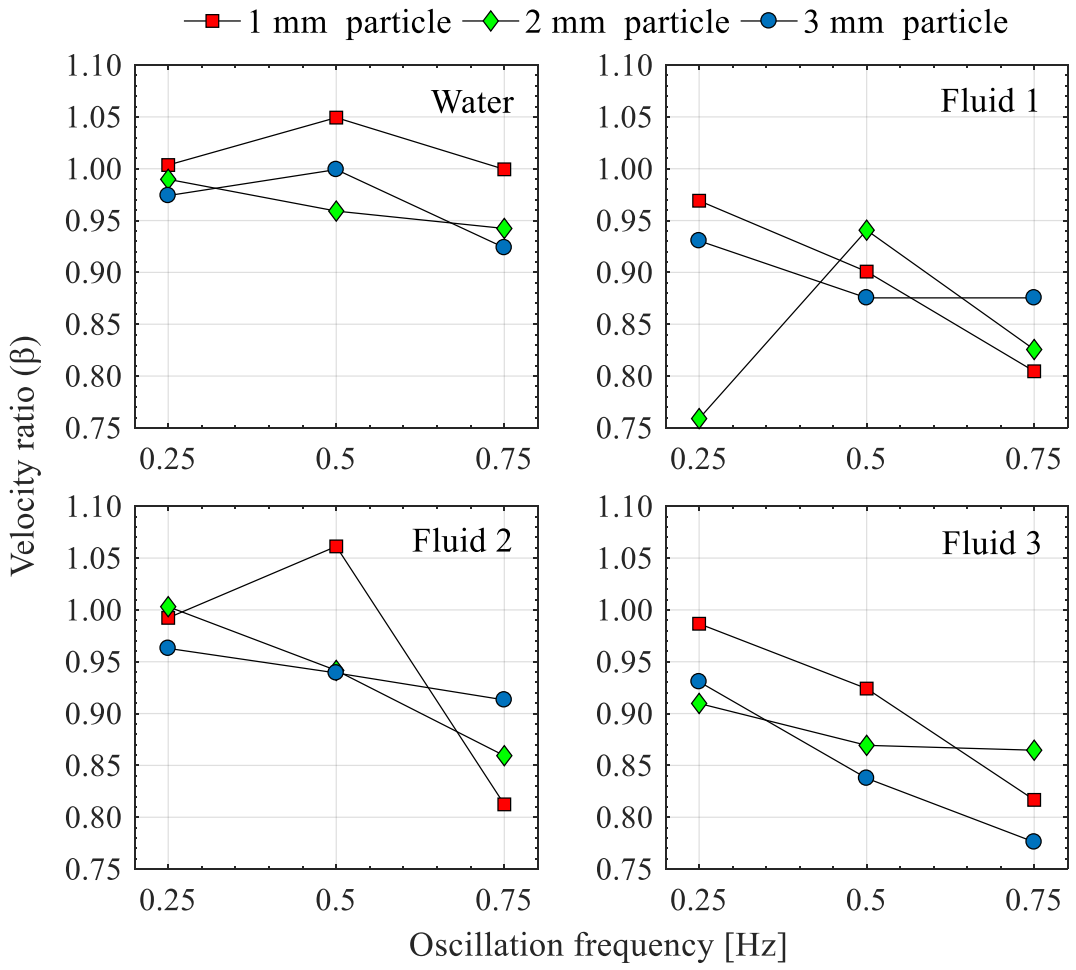

Fig. 12. Variation of β at different oscillation frequencies for different particle sizes.

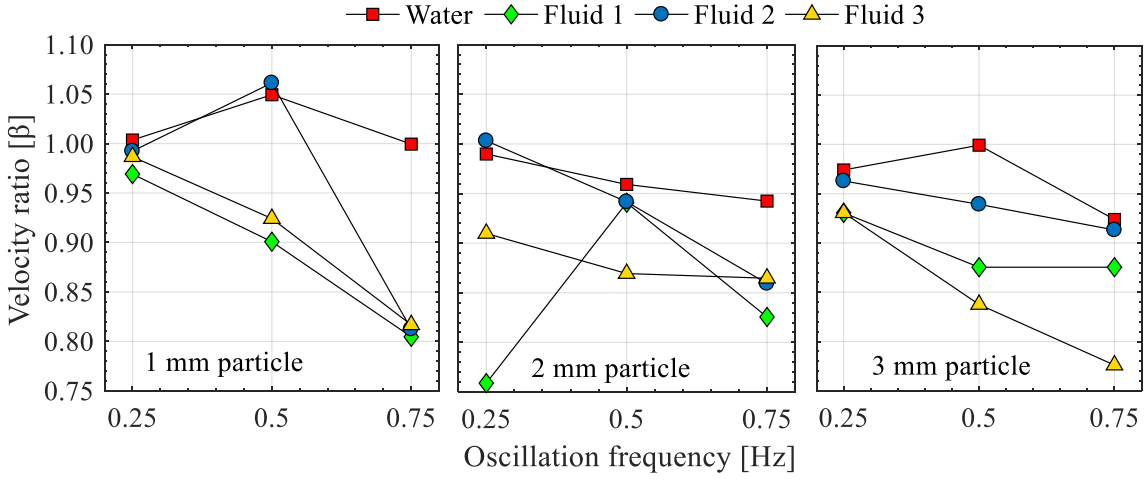

Fig. 13. Variation of β at different oscillation frequencies in different fluid types.

3.5.1. Wall effects at stationary conditions

When a spherical particle settles within some confined walls, it experiences a retardation effect and reduces its settling velocity. This effect is quantified in terms of a wall factor (Malhotra and Sharma, 2012) which is defined as the ratio of the settling velocity in the presence of confining walls to the unbounded settling velocity in the same fluid. The presence of walls generally creates an enhancement of the drag force (Zeng et al., 2009), and more importantly the particle experiences a lift force that is either directed toward or away from the wall. This lift force (Fischer et al., 2002) is often much smaller in magnitude than the drag force and plays a vital role in determining the solids separation or suspension capacities in many industrial applications. Authors have investigated the wall effects on particle settling at steady conditions and Fig. 13 shows the velocity ratio at different locations where β at 'L1' always reads as unity based on the definition of β in Eq. (14).

According to Fig. 14, it can be seen that the wall effects are

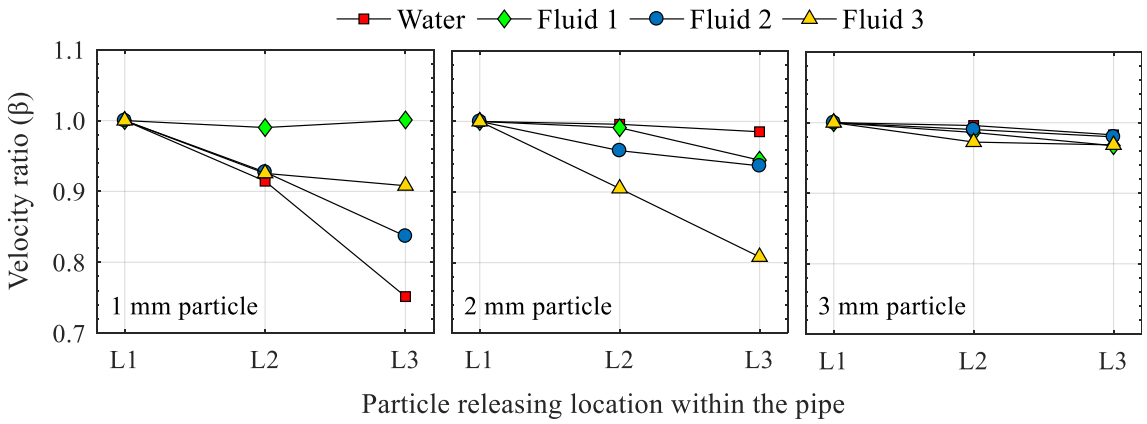

Fig. 14. Wall effects on particle settling at steady conditions in different fluid types.

significant when smaller sized particles settle in both Newtonian and non-Newtonian fluids. When a 1 mm particle settles in water, β shows a reduction of around 25% while it is just around 3% when a 3 mm particle settles in water.

Furthermore, it is observed that the wall retardation becomes less significant when the non-Newtonian fluids become more viscous and it becomes less severe in power-law fluids than in Newtonian fluids. The outliers in the experimental data points presented in Fig. 14 could be attributed to the transverse (lift) force that is directed away from the wall at those particular instances. According to (Zeng et al., 2005, 2009), when the *Re* becomes higher (around 200), a more pronounced one-sided double-threaded wake could be observed between the particle and the wall. Furthermore, when the particle becomes closer and closer to the wall, the recirculation region opposite of the wall and the vorticity are significantly larger than that within the gap between the particle and the wall which will eventually increase the drag force on the particle. However, the effect of particle size on oscillation-induced retardation is more significant than that observed for the wall-effect in the absence of

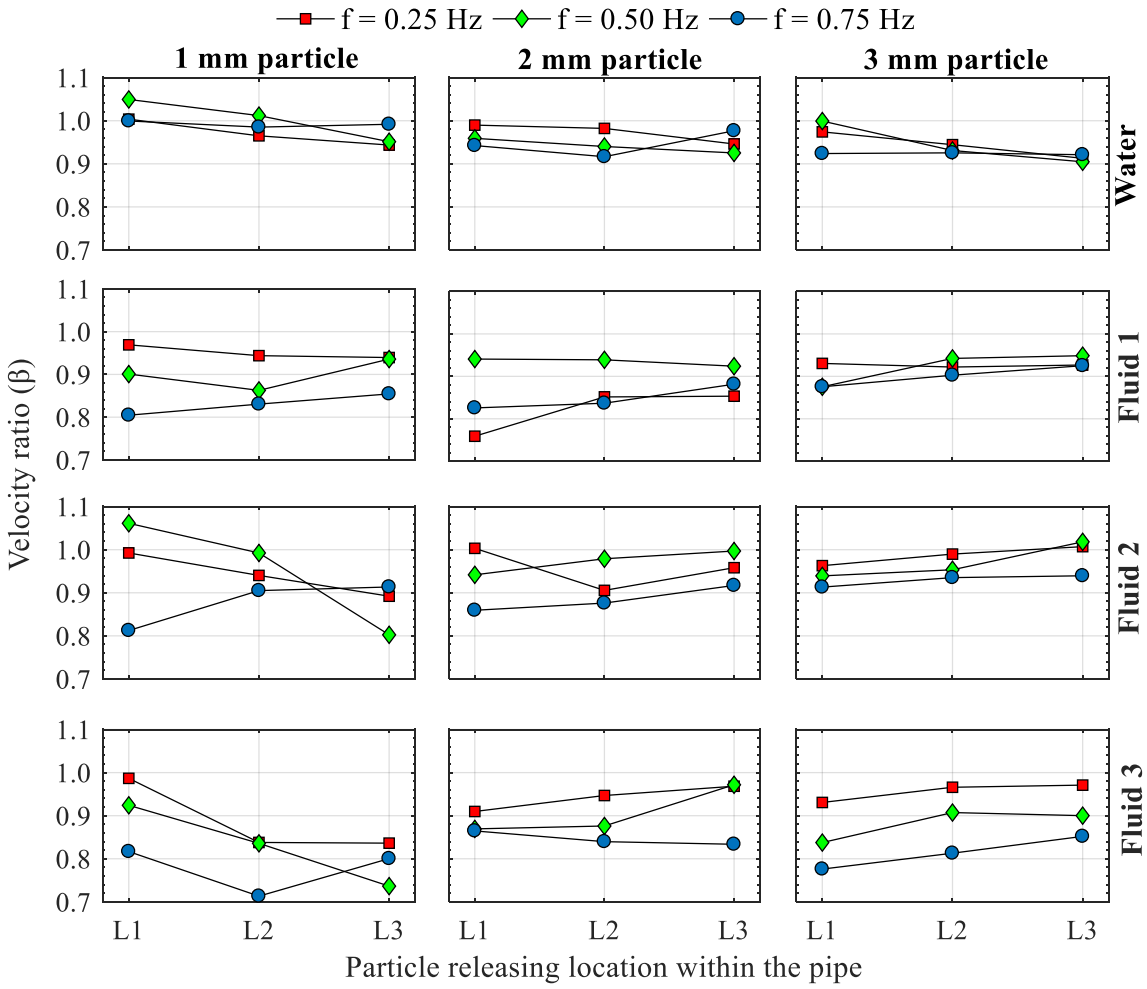

Fig. 15. Effect of the shear region on particle settling at oscillatory conditions in different fluid types.

oscillation.

3.5.2. Effect of the shear region at oscillatory conditions

In comparison to the wall-effects at stationary conditions, a particle which moves parallel to a wall in an oscillatory flow behaves in a slightly different manner since it does not experience a transverse (lift) force at least within the Stokes region (Zeng et al., 2009). However, with the introduction of the inertial effects in oscillatory flow, the lift force has three contributions from the shear flow, from the rotation itself and from the wall where it is bounded. The relative motion of the surrounding liquid and the particle within the gap between the particle and the wall contributes to this inward or outward lift forces which can be significant when the flow becomes more inertia dominated (high *Re*). Fig. 15 shows how the velocity ratio (β) varies when the particle can settle closer to the pipe wall in oscillatory conditions.

It could be seen that when the particle is close to the wall in water, β tends to reduce. But, when it is allowed to settle in non-Newtonian fluids closer to the wall and at oscillating conditions, β tends to show a slight increase. This slight increase may not be sufficient to overcome the terminal settling velocity at stationary conditions, but that is considerable and interesting to study since it is expected to have an increased drag as a result of both shear flow and the wall-effect. Despite the slight anomalies shown by the 1 mm particle from the above-mentioned observation, 2 mm and 3 mm particles are in good agreement. Such slight anomalies shown by the 1 mm particle could be attributed to the irregularities of the shape and size of the particle and also the break-neck effects exerted by the mechanical oscillatory system to the fluid medium. The slight increase in β could be attributed to the increased shear effects and the slight drag reduction within the Stokes region (Zeng et al., 2005, 2009) in the presence of the oscillations, which can be elucidated as follows.

The viscosity of most water-based drilling fluids is formulated by a combination of polymers similar to the test fluids in the current study. Besides, water-based drilling fluids may contain some additives to achieve desired agglomeration effects. The structural units and surface charges between those particles in polymeric liquids may get weakened by the oscillations/vibrations and that leads to a reduction of internal liquid viscosity. It is to be noted that the cyclic maximum shear rate change occurs mostly near the pipe wall, and thus the resulting viscosity reduction is more pronounced in the near-wall regions (Amaratunga et al., 2020). This explains the fact that, when the shear-thinning non-Newtonian fluids (primarily water-based polymeric liquids) are subjected to oscillatory motion, there will be a substantial reduction of viscosity of the fluid and that will result in the reduction of the drag force on the settling particles and consequently experiences faster settling. Furthermore, it is important to know that there exist some interactions of the particle with the coherent vortex structures in the near-wall region as explained by (Mazzuoli et al., 2014) and the hydrodynamic force on the sphere is characterized by such complex time development. Since the particles are released fairly close to the wall at L3, their trajectory (and thus the average velocity) is largely influenced by the vorticity present in the vicinity of the wall. Vortices are generated in the boundary layer during some positions of the oscillation period.

Therefore, the non-linear dependence of the drag force on the relative velocity of the particle to fluid becomes apparent in the presence of oscillatory motion since the shear effects come into action and the shear rate increases closer to the walls. It can be concluded that the mean relative velocity of settling (or rising) of particles in a liquid medium is reduced if the liquid medium is made to undergo sinusoidal vertical oscillations. However, the settling particles in that oscillating fluid medium closer to the pipe wall would experience a slight reduction in drag within the shear region than that in the core region.

3.6. Error analysis

As stated previously, it is important to discuss the error associated with the current analysis since it contains some approximations in averaging the settling velocity at oscillatory conditions, which is the significant parameter in the present study. The error sources associated with this study could be two-fold; namely, (i) the experimental (or the random) error when capturing the position of the settling particle and (ii) the error associated with approximating the slope for the displacement profile of the particles when they are settling in oscillatory conditions. In a way, the latter could be considered as a 'systematic' error since it is obvious to deviate from the linear curve. On the other hand, the size of the particles is not exactly 1, 2, or 3 mm (as shown in Table 2) could also be a slight contribution to the systematic error of the experiment. However, it is of great importance to mention here that, the vertical displacement of the particles has been recorded for a time long enough to estimate the average slope with precision. The authors wanted to investigate the behavior of the falling particle throughout its whole path within the test section rather than just calculating the average velocity at the bottom of the test section as 'a specified distance divided by the time spent'.

To assess the associated error and to enhance the accuracy of results, all the experimental cases were repeated three times. Out of those trials, it could be observed that the terminal settling velocities at stationary conditions has the lowest standard deviation of 0.000437 m/s when 3 mm particle settles in Fluid 3 and the largest standard deviation of 0.0387 m/s when 1 mm particle settles in water. Even for the oscillatory cases, the random error was not significant in such a way that their standard deviations are comparably too small. This indicates that the random error which is associated with the results of this particular study would be not that significant.

Furthermore, when approximating the slope for the displacement profile of the particles under oscillatory conditions, some cases exhibited significant deviations as shown in Fig. 16. It can be seen that R^2 values are within the acceptable range (>90%) for still fluids, and also when they oscillated at very low frequencies. Further increase in the frequency enhances the deviation especially for the smaller sized particles when they are settling in highly viscous non-Newtonian fluids. The lowest R^2 values recorded are around 17% when 1 mm particle settles in Fluid 3. As stated in section 3.3.2, the condition of partial stability or the temporary stagnation of the particles within its course of settling is the closest reason for this increased deviation (or lower R^2 value) for smaller-sized particles in high viscous non-Newtonian fluids. As earlier mentioned, it was found to have certain oscillation frequencies where the absolute downward displacement of the particle is smaller than its displacement in the opposite direction, regardless of the gravitational force. And so, the displacement profile of the particle also showed more or less sinusoidal pattern which consequently reduces the R^2 value of the fitted linear curve. The authors understand the necessity of performing more tests for each experimental condition to achieve better convergence statistics and a comprehensive investigation would require observing the velocity field around the particle during its motion, for instance utilizing PIV measurements.

However, taking the average settling velocity even with such low R^2 values were successful in quantifying the oscillation-induced reduction of settling velocity of particles in Newtonian and non-Newtonian fluids.

4. Conclusion

This experimental investigation was carried out to study the effects of oscillatory motion on the settling of spherical particles in Newtonian and slightly viscoelastic non-Newtonian fluids. 144 different experimental cases were tested for 3 different frequencies and still fluid, 3 different particle sizes, 4 different fluid types, and 3 different locations within the pipe. The study concludes that;

- Oscillations lead to increased drag force exerted on the settling particles in both Newtonian and non-Newtonian fluids.

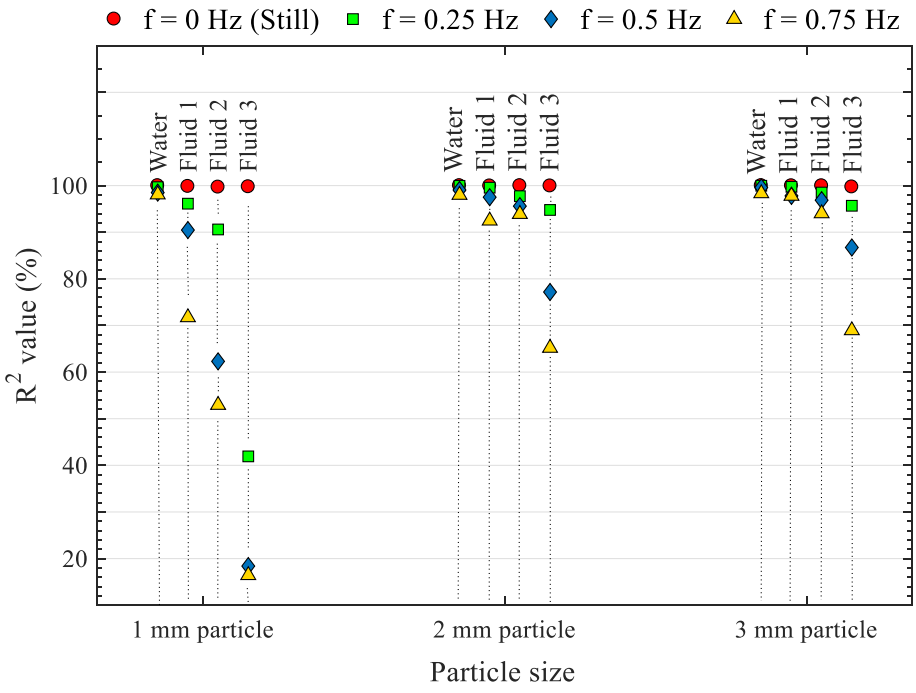

Fig. 16. Resulted R^2 value in approximating the slope for the displacement profiles of particles in oscillatory conditions.

- The increased drag effect becomes significant in stagnant conditions when the non-Newtonian fluids are more viscous and shear-thinning. This reduction of terminal settling velocity could also be attributed to the negative wake that is perceived to happen only in shear-thinning viscoelastic fluids.
- In quiescent fluids, the rate of increase in terminal settling velocity (with increasing particle size) is higher for water and low viscous NNFs compared to that in high viscous NNFs. This means that larger particles settle down at a slower rate than the smaller particles when the shear-thinning of the NNF is increasing (when n becomes low). Therefore, increasing shear viscosity may be an effective solution to achieve suspensions of large-sized particles.
- A condition of partial stability of the particles within its course of settling could be observed in some instances especially at higher fluid viscosities and also for smaller sized particles under oscillatory conditions. Such temporary stable condition could be seen only when the fluid medium moves upward in its oscillating period due to the neutralization of finite buoyancy forces by the gravitational and drag forces acting on the particle.
- The settling velocity of particles in both Newtonian a non-Newtonian fluids experiences reduction under oscillatory conditions. This reduction of settling velocity may be primarily related to increased drag forces induced by the fluid oscillations.
- Velocity retardation effect under oscillatory conditions becomes significant by reduction of the power-law index, *n* and with relatively large-sized particles.
- The impact of wall retardation at steady conditions becomes less significant when the non-Newtonian fluids become more viscous and it becomes less severe in power-law fluids than in Newtonian fluids.
- The effect of particle size on oscillation-induced retardation is more significant than that observed for the wall-effect in the absence of oscillation.
- When the shear-thinning non-Newtonian fluids (primarily water-based polymeric liquids) are exposed to oscillatory motion, there will be a reduction of viscosity of the fluid closer to the pipe walls where the shear region exists and that will result in the reduction of the drag force on the settling particles.
- Even though the approximation of average settling velocity from particle displacement profile (as described in section 2.3.2) seems less accurate in some instances, it is a successful way in quantifying the oscillation-induced retardation of settling velocity of particles in Newtonian and non-Newtonian fluids.

As an overall idea, the analysis presented in this manuscript reveals that an enhancement of suspension and mixing in both Newtonian and non-Newtonian fluids could occur in oscillatory flows. However, when particles are moving close to the pipe wall in oscillatory shear-thinning non-Newtonian fluid medium, they experience a slight reduction in drag compared with the Newtonian case. The shear rate at equivalent flow rate is higher in shear-thinning liquids close to the wall, thus the effective viscosity is reduced. Furthermore, the authors expect that this work will stimulate further experimentation on different aspects especially in understanding the hydrodynamics forces on the particles being settled in oscillatory non-Newtonian fluids.

CRediT authorship contribution statement

Maduranga Amaratunga: Conceptualization, Methodology, Software, Validation, Formal analysis, Investigation, Resources, Data curation, Writing - original draft, Writing - review & editing, Visualization. **Herimonja A. Rabenjafimanantsoa:** Methodology, Formal analysis, Investigation, Resources, Writing - original draft, Writing - review & editing, Visualization, Supervision, Project administration, Funding acquisition. **Rune W. Time:** Conceptualization, Formal analysis, Resources, Data curation, Writing - original draft, Writing - review & editing, Supervision, Project administration, Funding acquisition.

Declaration of competing interest

The authors declare that they have no known competing financial interests or personal relationships that could have appeared to influence the work reported in this paper.

Acknowledgment

Authors gratefully acknowledge the Norwegian Research Council for funding this study under the project "NFR Improved Model Support in Drilling Automation". We appreciate the valuable support provided by Jon Arne Evjenth, from the Department of Energy & Petroleum Engineering at the University of Stavanger in preparing the data acquisition system for the experiments. The advice and encouragement provided by Roar Nybø and Knut S. Bjørkevoll from SINTEF, Bergen are also greatly appreciated.

Appendix A. Supplementary data

Supplementary data to this article can be found online at https://doi.org/10.1016/j.petrol.2020.107786.

References

Acharya, A.R., 1986. Particle transport in viscous and viscoelastic fracturing fluids. SPE Prod. Eng. 1, 104–110.
Amaratunga, M., Nybø, R., Time, R.W., 2018. PIV analysis of dynamic velocity profiles in non-Newtonian drilling fluids exposed to oscillatory motion. ASME 2018 37th International Conference on Ocean, Offshore and Arctic Engineering. American Society of Mechanical Engineers Digital Collection.
Amaratunga, M., Rabenjafimanantsoa, H.A., Time, R.W., 2019a. CFD Analysis of low frequency oscillations in Newtonian and non-Newtonian fluids in a vertical pipe. WIT Trans. Eng. Sci. 125, 37–48.
Amaratunga, M., Rabenjafimanantsoa, H.A., Time, R.W., 2019b. Comparison of oscillatory flow conditions in Newtonian and non-Newtonian fluids using PIV and high-speed image analysis. Flow Meas. Instrum. 70, 101628.
Amaratunga, M., Rabenjafimanantsoa, H.A., Time, R.W., 2020. Estimation of shear rate change in vertically oscillating non-Newtonian fluids. Predict. Partic. Settl. 277, 104236.
Arnipally, S.K., Kuru, E., 2018. Settling velocity of particles in viscoelastic fluids: a comparison of the shear-viscosity and elasticity effects. SPE J. 23 (5) https://doi.org/10.2118/187255-PA.
Bailey, J., 1974. Particle motion in rapidly oscillating flows. Chem. Eng. Sci. 29, 767–773.
Baird, M., Senior, M., Thompson, R., 1967. Terminal velocities of spherical particles in a vertically oscillating liquid. Chem. Eng. Sci. 22, 551–558.
Becker, L., Mckinley, G., Rasmussen, H.K., Hassager, O., 1994. The unsteady motion of a sphere in a viscoelastic fluid. J. Rheol. 38, 377–403.
Boyadzhiev, L., 1973. On the movement of a spherical particle in vertically oscillating liquid. J. Fluid Mech. 57, 545–548.
Brown, P.P., Lawler, D.F., 2003. Sphere drag and settling velocity revisited. J. Environ. Eng. 129, 222–231.
Cheng, N.-S., 2009. Comparison of formulas for drag coefficient and settling velocity of spherical particles. Powder Technol. 189, 395–398.
Cherukat, P., Mclaughlin, J.B., 1994. The inertial lift on a rigid sphere in a linear shear flow field near a flat wall, 263, 1–18.
Chhabra, R., Agarwal, L., Sinha, N.K., 1999. Drag on non-spherical particles: an evaluation of available methods. Powder Technol. 101, 288–295.
Childs, L., Hogg, A., Pritchard, D., 2016. Dynamic settling of particles in shear flows of shear-thinning fluids. J. Non-Newtonian Fluid Mech. 238, 158–169.
Clift, R., Grace, J.R., Weber, M.E., 1978. Bubbles, Drops, and Particles. Academic Press, New York, p. 1978.
Fischer, P.F., Leaf, G.K., Restrepo, J.M., 2002. Forces on particles in oscillatory boundary layers, 468, 327–347.
Gheissary, G., Van Den Brule, B., 1996. Unexpected phenomena observed in particle settling in non-Newtonian media. J. Non-Newtonian Fluid Mech. 67, 1–18.
Haider, A., Levenspiel, O., 1989. Drag coefficient and terminal velocity of spherical and nonspherical particles. Powder Technol. 58, 63–70.
Harbaum, K., Houghton, G., 1960. Effects of sonic vibrations on the rate of absorption of gases from bubble beds. Chem. Eng. Sci. 13, 90–92.
Harrington, L.J., Hannah, R.R., Williams, D., 1979. Dynamic experiments on proppant settling in crosslinked fracturing fluids. SPE Annual Technical Conference and Exhibition. Society of Petroleum Engineers.
Herringe, R., 1976. On the motion of small spheres in oscillating liquids. Chem. Eng. J. 11, 89–99.
Herringe, R., Flint, L., 1974. Particle motion in vertically oscillated liquids. Fish Australian Conference on Hydraulics and Fluid Mechanics, pp. 103–110.
Houghton, G., 1963. The behaviour of particles in a sinusoidal velocity field. Proc. Roy. Soc. Lond. Math. Phys. Sci. 272, 33–43.
Houghton, G., 1966. Particle trajectories and terminal velocities in vertically oscillating fluids. Can. J. Chem. Eng. 44, 90–95.
Houghton, G., 1968. Particle retardation in vertically oscillating fluids. Can. J. Chem. Eng. 46, 79–81.
Hwang, P.A., 1985. Fall velocity of particles in oscillating flow. J. Hydraul. Eng. 111, 485–502.
Ikeda, S., Yamasaka, M., 1989. Fall velocity of single spheres in vertically oscillating fluids. Fluid Dynam. Res. 5, 203.
Jin, L., Penny, G.S., 1995. Dimensionless methods for the study of particle settling in non-Newtonian fluids. J. Petrol. Technol. 47, 223–228.
Kehlenbeck, R., Felice, R.D., 1999. Empirical relationships for the terminal settling velocity of spheres in cylindrical columns. Chem. Eng. Technol.: Ind. Chem. Plant Equip. Process Eng. Biotechnol. 22, 303–308.
Kelessidis, V.C., 2004. An explicit equation for the terminal velocity of solid spheres falling in pseudoplastic liquids. Chem. Eng. Sci. 59, 4437–4447.
Khan, A., Richardson, J., 1987. The resistance to motion of a solid sphere in a fluid. Chem. Eng. Commun. 62, 135–150.
Lee, H., Balachandar, S.J., 2010. Drag and lift forces on a spherical particle moving on a wall in a shear flow at finite Re, 657, 89–125.
Maalouf, A., Sigli, D., 1984. Effects of body shape and viscoelasticity on the slow flow around an obstacle. Rheol. Acta 23, 497–507.
Malhotra, S., Sharma, M.M., 2012. Settling of spherical particles in unbounded and confined surfactant-based shear thinning viscoelastic fluids: an experimental study. Chem. Eng. Sci. 84, 646–655.
Mazzuoli, M., Kidanemariam, A.G., Uhlmann, M.J., 2019. Direct numerical simulations of ripples in an oscillatory flow, 863, 572–600.
Mazzuoli, M., Seminara, G., Vittori, G.J., 2014. Settling of heavy particles in a turbulent Stokes layer: numerical simulations, 72, 2–14.
Morrison, F.A., 2013. An Introduction to Fluid Mechanics. Cambridge University Press.
Morrison, F.A., 2016. Data correlation for drag coefficient for sphere. https://pages.mtu.edu/~fmorriso/DataCorrelationForSphereDrag2016.pdf.
Schöneborn, P.-R., 1975. The interaction between a single particle and an oscillating fluid. Int. J. Multiphas. Flow 2, 307–317.
Shah, S.N., 1982. Proppant settling correlations for non-Newtonian fluids under static and dynamic conditions. Soc. Petrol. Eng. J. 22, 164–170.
Shah, S.N., 1986. Proppant-settling correlations for non-Newtonian Fluids. SPE Prod. Eng. 1, 446–448.
Shah, S.N., El Fadili, Y., Chhabra, R., 2007. New model for single spherical particle settling velocity in power law (visco-inelastic) fluids. Int. J. Multiphas. Flow 33, 51–66.
Sharma, H., 1979. Creeping motion of a non-Newtonian fluid past a sphere. Indian J. Pure Appl. Math. 10, 1565.
Singh, S.P., Srivastava, A.K., Steffe, J.F., 1991. Vibration induced settling of a sphere in a Herschel-Bulkley fluid. J. Food Eng. 13, 181–197.
Still, A., 2012. Multiphase Phenomena in a Vibrating Column Reactor. Oklahoma State University.
Talmon, A., Huisman, M., 2005. Fall velocity of particles in shear flow of drilling fluids. Tunn. Undergr. Space Technol. 20, 193–201.
Time, R.W., Rabenjafimanantsoa, A., 2013. On the relevance of laboratory scale rheometric measurements for calculation of complex large scale flows in well drilling and pipe flows. Ann. Trans. Nordic Rheol. Soc. 22.
Tunstall, E., Houghton, G., 1968. Retardation of falling spheres by hydrodynamic oscillations. Chem. Eng. Sci. 23, 1067–1081.
Uhlherr, P., Le, T., Tiu, C.J., 1976. Characterisation of inelastic poweriaw fluids using falling sphere data, 54, 497–502.
Uhlmann, M., Dušek, J., 2014. The motion of a single heavy sphere in ambient fluid: a benchmark for interface-resolved particulate flow simulations with significant relative velocities, 59, 221–243.
Van Den Brule, B., Gheissary, G., 1993. Effects of fluid elasticity on the static and dynamic settling of a spherical particle. J. Non-Newtonian Fluid Mech. 49, 123–132.
Zeng, L., Balachandar, S., Fischer, P.J., 2005. Wall-induced forces on a rigid sphere at finite Reynolds number, 536, 1–25.
Zeng, L., Najjar, F., Balachandar, S., Fischer, P., 2009. Forces on a finite-sized particle located close to a wall in a linear shear flow, 21, 033302.
Zhiyao, S., Tingting, W., Fumin, X., Ruijie, L., 2008. A simple formula for predicting settling velocity of sediment particles. Water Sci. Eng. 1, 37–43.